

Vortex ground state for small arrays of magnetic particles with dipole coupling

S. A. Dzian,¹ A. Yu. Galkin,² B. A. Ivanov,^{1,3,*} V. E. Kireev,³ and V. M. Muravyov³

¹*Radiophysics Department, National Taras Shevchenko University of Kiev, 03127 Kiev, Ukraine*

²*Institute of Metal Physics, 03142 Kiev, Ukraine*

³*Institute of Magnetism, 03142 Kiev, Ukraine*

(Received 21 January 2013; published 8 May 2013)

We show that a magnetic vortex is the ground state of an array of magnetic particles shaped as a hexagonal fragment of a triangular lattice, even for a small number of particles in the array $N \leq 100$. The vortex core appears and the symmetry of the vortex state changes with the increase of the intrinsic magnetic anisotropy of the particle β ; the further increase of β leads to the destruction of the vortex state. Such vortices can be present in arrays as small in size as a dozen nanometers.

DOI: [10.1103/PhysRevB.87.184404](https://doi.org/10.1103/PhysRevB.87.184404)

PACS number(s): 75.10.Hk, 75.50.Tt, 75.30.Kz

I. INTRODUCTION

Topological defects of vortex type play a paramount part in the general physics of ordered media such as superfluidity, superconductivity, and magnetism. In particular, vortices and vortex pairs are important in two-dimensional (2D) magnetism. Recently, the ground state of soft ferromagnetic particles of micron and submicron size has been shown to be of the vortex type, which has received much attention from the research community.^{1–3} Compared to vortices in superfluid systems, magnetic vortices in 2D ferromagnets and antiferromagnets have a richer behavior since they may be divided into two different classes, in-plane and out-of-plane vortices.^{4,5} For in-plane vortices all spins lie in the vortex plane. Out-of-plane vortices have nonzero spin components orthogonal to the vortex plane localized within the so-called *vortex core*, a small region near the vortex center. Vortices with a core are described by several different types of topological charges.^{6–8} Besides the standard π_1 topological charge *vorticity* q , which is similar to *circulation* in a supercurrent systems, one can introduce a π_2 topological charge, the *polarity* or *polarization* $p = \pm 1$ of the vortex core, which is the spin direction in the core and is connected to the π_2 topological charge of the magnetization field. In-plane vortices can be associated with the value $p = 0$. Further, vortices found in the ground state of soft magnetic particles should have $q = 1$ only ($q = -1$ corresponds to antivortices that can be connected to “antidots,” small holes in a patterned magnetic film⁹), but they are additionally classified by the discrete number *chirality* $C = \pm 1$, which is the sense of rotation of magnetization far from the vortex core. For a single vortex in a bulk 2D magnet with easy-plane magnetic anisotropy, there is a transition from coreless in-plane vortex structure to the vortex with a well-defined core, as the anisotropy strength decreases below a certain critical value.¹⁰ The presence of a core plays a crucial role in the dynamic properties of magnetic vortices. In particular, the value of the π_2 topological charge determines special gyroscopic properties of the vortex dynamics and the presence of low-frequency dynamics, as well as the splitting of doublets for modes with nonzero azimuthal number, either for the easy-plane local model^{4,11} or for the vortex-state soft magnetic dots where the dipolar interaction prevails.^{12–16} For the vortex-state magnetic dots, the main features of the normal modes were experimentally observed by means of

different technique^{14,17–22} (see also Refs. 2 and 3 for a review.) The vortex-state dots and their spin dynamics are essential for possible applications of magnetic vortices in perspective spintronic^{23–30} and magnonic^{31,32} devices.

The presence of vortices in the ground state of soft ferromagnetic particles is determined by the balance between magnetostatic and exchange energies. For disk-shaped particles with negligible magnetocrystalline anisotropy and typical thicknesses about 20–50 nm, the vortex state is stable if the disk radius exceeds some critical value $R_c \sim 150\text{--}200$ nm. Vortices in the ground state of soft magnetic particles possess a well-developed core with a size of the order of the exchange length of the material (about 15 nm in Permalloy). It has been recently shown that magnetic vortices of different structures can be the ground state for magnetic particles with comparable energies of the exchange and dipolar interactions, even for a small (of the order of 10^3) number of magnetic moments in the particle.³³ A highly nonuniform ground state is found for small particles with a sufficiently high surface anisotropy as well.^{34,35}

From the perspective of a search for vortex states, the promising magnetic systems are those in which the exchange interaction is suppressed or nonexistent, and the main source of interaction among structural elements is the dipole-dipole interaction of their magnetic moments. These are so-called *dipolar magnets*, i.e., such spin systems where a long-range magnetic dipole interaction prevails. Dipolar magnets have been attracting persistent interest in recent decades as objects of the fundamental physics of magnetism possessing some unusual properties. One may mention the presence of an ambiguous ground state with nontrivial continuous degeneracy even for simple cubic^{36,37} or 2D square lattices^{38–40} and the existence of special phase transitions induced by an external magnetic field.^{41,42} Magnon spectra of such systems have nonanalytic behavior at small wave vectors.^{43–48}

The interest in systems with dominant magnetic dipole interaction has significantly increased in recent years, mainly in the context of artificial magnetic materials such as arrays of magnetic nanoparticles.¹ Magnetic systems with dominant dipole interaction possess interesting physical properties important for applications. Among those properties, one can highlight the fact that the ground state of an infinite system of magnetic moments constituting a lattice and coupled by

the dipole-dipole interaction depends essentially on the lattice structure,⁴⁰ and in the presence of the intrinsic (intraparticle) anisotropy it depends on the orientation of the easy axis of this anisotropy with respect to the lattice axes as well.

Let us discuss 2D lattices, which will be the object of our study. For lattices of particles with a high perpendicular anisotropy, the ground state corresponds to various types of two-sublattice antiferromagnetic order; particularly, a chess-board structure is realized for a square lattice,⁴¹ and a layered one is realized for a triangular lattice.⁴⁹ For finite fragments of such lattices these structures vary insignificantly compared to the infinite case. In the case of systems with an in-plane anisotropy, the role of the boundaries is more essential. For an infinite square lattice, the ground state has four-sublattice antiferromagnetic order and has a high (continuous) degeneracy, while for the triangular lattice a ferromagnetic order is realized.⁴⁰ The presence of a boundary, however, may change significantly the state of such a system. For finite fragments of the square lattice the aforementioned continuous degeneracy is removed, but the state remains antiferromagnetic.^{42,50} For a triangular lattice of dipoles, the state changes are more radical, and in finite samples the ground state can be a vortex state with a closed flux of magnetization formed by the magnetic moments lying in the plane of the array.⁵¹ In general, the reason for the emergence of vortices is the same as for soft magnetic dots⁵² (see also Refs. 1–3), where the vortex state emerges due to the energy gain of the closure of magnetic flux in the sample, and the vortices are an alternative to a standard domain structure. However, for a rectangular-shaped array the vortex state is advantageous only for large enough arrays.⁵¹

In view of the importance of vortices for the fundamental physics of magnetism as well as for a variety of applications, searching for physical systems with a vortex-type ground state is of great interest. In particular, the minimal size of a system carrying a vortex is interesting, along with whether that size can be made significantly smaller than the critical size R_c indicated above.

In this paper, we will demonstrate that for an array of particles shaped as a fragment of a triangular lattice with high hexagonal symmetry (see Fig. 1), the ground state is a vortex state even for a small number of particles in the array. Even for an extremely small array of this type, which consists of seven particles, the vortex-state energy is almost two times lower

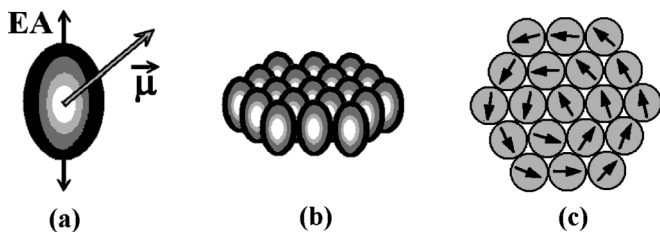


FIG. 1. The model of a planar array of magnetic nanoparticles. (a) The shape of a single elongated magnetic particle; the easy axis is denoted EA, and the orientation of the magnetic moment $\vec{\mu}$ is denoted by the arrow. (b) A symmetric plane cluster comprised of 19 particles. (c) The same in a plane view; magnetic moments of particles in a planar vortex existing at small anisotropy are shown with arrows.

than that of a quasihomogeneous state. We show further that such arrays have very interesting behavior: their ground-state structure is highly sensitive to the change of the anisotropy of a single particle. In particular, for a particle made of a soft magnetic material this anisotropy could be varied by changing the particle shape.

II. MODEL AND RESULTS

Consider an array of particles placed at the sites of a finite hexagonally shaped fragment of a 2D triangular lattice. The energy of the this system contains contributions from the energy of the magnetic dipole interaction and from the energy of the anisotropy:

$$W = \frac{1}{2} \sum_{\vec{l} \neq \vec{l}'} \frac{\vec{\mu}_{\vec{l}} \vec{\mu}_{\vec{l}'} - 3(\vec{\mu}_{\vec{l}} \vec{v})(\vec{\mu}_{\vec{l}'} \vec{v})}{|\vec{l} - \vec{l}'|^3} + \frac{\beta}{a^3} \sum_{\vec{l}} [(\vec{\mu}_{\vec{l}} \cdot \vec{e}_x)^2 + (\vec{\mu}_{\vec{l}} \cdot \vec{e}_y)^2], \quad (1)$$

where $\vec{\mu}_{\vec{l}}$ is the magnetic moment of the particle at site \vec{l} , $|\vec{\mu}| = \mu_0$, μ_0 is the magnetic moment of a single particle, $\vec{v} = (\vec{l} - \vec{l}')/|\vec{l} - \vec{l}'|$, a is the lattice constant (the distance between closest particles in the array plane), and β is a dimensionless constant determining the magnetic anisotropy strength of a particle. This anisotropy is assumed to be uniaxial, of the easy-axis type (so that $\beta > 0$), with the easy axis \vec{e}_z perpendicular to the system plane. Here $\vec{e}_{x,y,z}$ are unit vectors along the coordinate axis.

One can expect that the absence or presence of a vortex core will depend on the effective anisotropy of the system. It is important to note that the total magnetic anisotropy of the array results from the uniaxial anisotropy of separate particles and from the easy-plane anisotropy of the array induced by the demagnetization field of a planar set of magnetic moments (similar to the shape anisotropy in the thin films). The competition of these two contributions determines the complex character of the distribution of magnetization in the array.

If the easy-plane anisotropy induced by the demagnetization field is sufficiently large, a suppression of the vortex core results. One can expect that the effective anisotropy can be changed by using magnetic particles possessing their own intrinsic easy-axis anisotropy. For the core to emerge, the effective anisotropy should be reduced, which takes place for particles with the easy axis perpendicular to the array plane. For arrays of particles made of soft magnetic materials, such a situation is realized in the case of elongated particles oriented perpendicular to the array plane (see Fig. 1). Such a geometry of the problem is promising for ultradense information storage^{53–55} and is naturally realized, for example, if the array is created by self-organization of small elongated particles floating in liquid. The competition of these two magnetic interactions provides the possibility to change the effective anisotropy of the system, which, as we will show below, allows one to impact the structure of the magnetic macrovortex.

To analyze this problem, we have employed two methods: numerical minimization of the energy (1) using the standard

Gauss-Seidel algorithm, as in Ref. 42, and Monte Carlo analysis using the simulated annealing technique.⁵⁶ The energy minimization has been performed as follows: we start with $\beta = 0$, choose a simple in-plane vortex as an initial condition, and numerically minimize the energy, and then the value of β is increased step by step. This method works pretty fast and gives a good description of the structure for continuous transitions (see below).

On the other hand, the Monte Carlo method with simulated annealing (MC-SA) is important for the analysis of points where the magnetic structure of the system changes discontinuously, with the coexistence of (metastable) states close to the transition point (see Ref. 56). In our case, this corresponds to the three-domain antiferromagnetic states as in Fig. 2(e). To find the global minimum of the energy of the system within this approach, first, the random initial configuration with all the magnetic moments perpendicular to the array's plane was selected. Every iteration of the MC-SA method consists of N moment reversal attempts on the random site, where N is the site number in the sample. The main idea of simulated annealing is that the probability of the reversal is nonzero even if the energy is increasing after this reversal; otherwise, the system with a high probability will be "frozen" in some local minimum. The probability depends not only on energy gain for reversal but also on a global time-varying parameter T called the *temperature*. If the reversal is favorable in energy, the moment is always reversed, irrespective of the temperature. But even if the reversal is unfavorable, the nonzero probability of reversal is chosen as follows: flip-over takes place if $Hm_0 < T|\log p|$, where T is the current value of the temperature and p is a random value generated in the range $0 < p \leq 1$. Here the parameter temperature determines the strategy of the minimization: for large T , the evolution is sensitive to coarser energy variations, while it is sensitive to finer energy variations when T is small. Thus the meaning of the temperature is the same as for annealing in metallurgy involving initial heating and controlled cooling of a material, thereby avoiding defect formation.

The temperature changes according to the quantity of full steps of MC-SA of the sample n as follows: $T = T_0 \min[\kappa, (n_0/n)^\alpha]$. Here the parameter T_0 was chosen as $(0.2-0.4)m_0^2/a^3$, and the cutoff parameter κ was equal to $\kappa = 3.0$ such that the initial temperature was high enough compared with the interaction energy. The optimal values of other parameter are defined by the trial runs; n_0 was equal to 10^4 to 5×10^4 , and the value of the α index was taken as $1/4$ or $1/5$. The temperature decreases with the process evolution, and magnetization reversals take place more rarely with decreasing energy. The process was stopped if the energy did not become less than the previous minimum during the previous $10n_0$ iterations. Then the next random configuration was generated, and the process was repeated. This analysis shows that the only three-domain antiferromagnetic configuration is present within all other possible states with perpendicular magnetic moments.

Numerical calculations have been carried out for comparatively small clusters shaped in the form of a regular hexagonal fragment of the lattice consisting of 19, 37, 61, 91, and 127 nanoparticles. For all studied systems, we have found an in-plane vortex in the ground state at small enough β . The

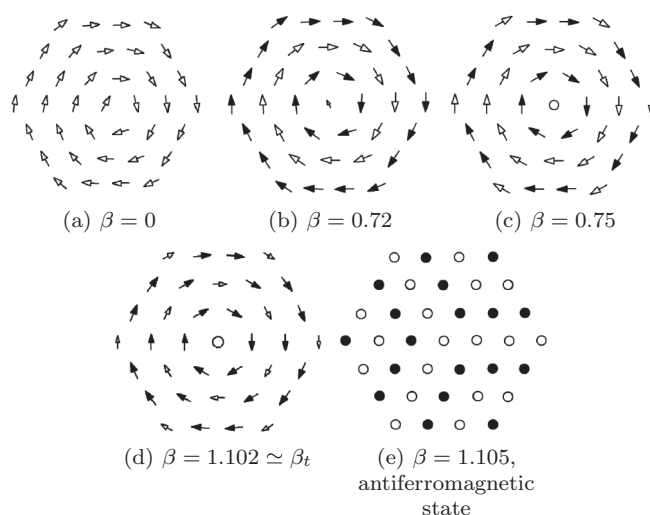


FIG. 2. Magnetic structure for the cluster of $N = 37$ particles at different values of the anisotropy constant β (here $\beta_1 = 0.697$, $\beta_2 = 0.729$); see the text. The planar components of the magnetic moments for each particle are shown with arrows, and vertical moments are represented by circles. For magnetic moments with positive or zero z projection, open symbols (arrows with open heads or open circles) are used, while particles with negative z projection of magnetic moments are depicted by the solid symbols.

structure of the vortex changes considerably as β increases and passes through two critical values, β_1 and β_2 ; see Fig. 2 and the detailed discussion below. Further, we have found a prominent transition at some value $\beta = \beta_t > \beta_{1,2}$ from the vortex state to the state with a fragment of the antiferromagnetic structure, and close to $\beta = \beta_t$ we have observed a noticeable region of coexistence of the vortex and antiferromagnetic states (see Fig. 3). The behavior of the energy as a function of the anisotropy constant β near this transition is similar to that for

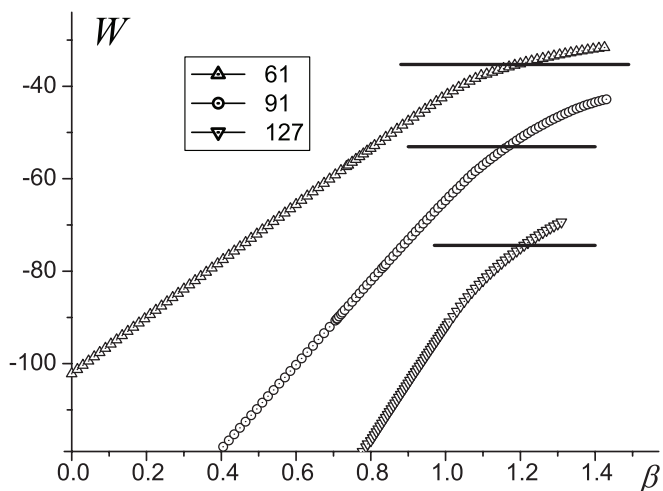


FIG. 3. The dependence of the energy W (in units of μ_0^2/a^3) on the anisotropy constant β for clusters of different sizes (labels in the legend denote the number of spins in the cluster), found by numerical minimization of (1). Horizontal lines denote the energy of three-domain antiferromagnetic state, see Fig. 2(e) while the symbols correspond to the energy of a vortex state.

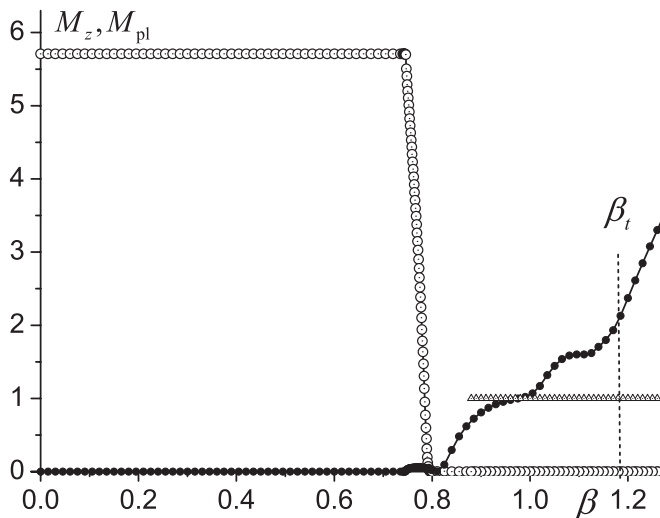


FIG. 4. The in-plane and out-of-plane magnetic moment components M_z (solid symbols) and M_{pl} (open symbols) vs the anisotropy constant β , in units of μ_0 , for a cluster with 61 particles. The details of behavior in the region of vortex core reconstruction, $\beta_1 < \beta_2 < \beta$ (here $\beta_1 \simeq 0.744$, $\beta_2 \simeq 0.786$), are presented in Fig. 5 on a different scale. Upward triangles label the value $M_z = \mu_0$ for the antiferromagnetic state.

a thermodynamic potential as a function of temperature near first-order phase transition. On the other hand, the dependence of the energy on β did not exhibit visible peculiarities at $\beta = \beta_{1,2}$, where a change of the vortex structure has been detected.

To analyze the structure and symmetry of the vortex core, after completing the energy minimization for each value of β , we have been calculating the value of the out-of plane component M_z of the total magnetic moment, as well as the length of the planar component $M_{pl} = \sqrt{M_x^2 + M_y^2}$. It turns out that just these parameters are most sensitive to the vortex structure and allow observing peculiarities of the vortex core behavior (see Fig. 4).

The behavior of the total magnetic moment of a particle array with a vortex is rather complicated. At small anisotropy, the picture remains the same as for isotropic particles,⁵¹ and a vortex with purely planar distribution of magnetic moments is realized. In this case, accordingly, the total z projection of the magnetic moment vanishes, but the planar component of the total magnetic moment M_{pl} is nonzero. With increasing β , a nonzero value of M_z emerges at some critical anisotropy $\beta = \beta_1$. The fact that $M_z \neq 0$ means that an out-of-plane core appears. However, with the appearance of nonzero M_z , the planar component of the total moment does not vanish immediately; i.e., within some finite interval $\beta_1 < \beta < \beta_2$ both in-plane and out-of-plane components of the moment are nonzero (see Figs. 4 and 5). The planar component vanishes for $\beta > \beta_2$, whereupon the vortex-state structure becomes more symmetric than that observed at $\beta < \beta_2$ (see Fig. 2). Such a symmetric vortex structure is observed within a wide range of β , $\beta_2 < \beta < \beta_t$, and the magnetic moment M_z changes considerably while M_{pl} remains zero. With the further increase of the anisotropy, the vortex structure becomes an antiferromagnetic structure similar to that found for strong perpendicular anisotropy. The presence of boundaries leads to

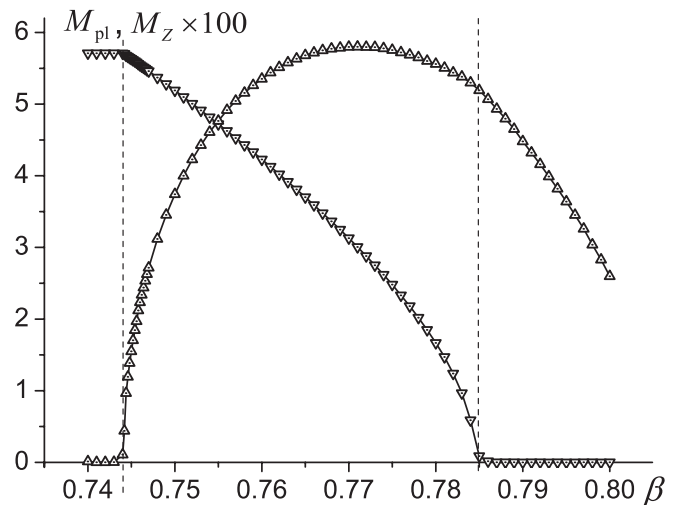


FIG. 5. The in-plane and out-of-plane magnetic moment components M_z (upward triangles) and M_{pl} (downward triangles) vs the anisotropy constant β , in units of μ_0 , for a cluster with 61 particles in the region of the vortex core reconstruction. Note that the scales for M_{pl} and M_z differ by a factor of 100.

the emergence of three different domains of such structure, as dictated by the system symmetry.

Note that the behavior of M_z and M_{pl} is similar to that of order parameters near second-order phase transitions. This observation can be used to perform a symmetry analysis of the transitions between the different vortex states. It is important to obtain analytical results due to the limited accuracy of numerical data and also because the numerical analysis is hindered near transition points $\beta = \beta_{1,2}$ because of the “critical slowing down” of relaxation similar to that found near a second-order phase transition, which manifests itself in a substantial increase in the numerical calculation time. Therefore we should study the possibilities of existence of such transitions in our system from the viewpoint of symmetry.

III. SYMMETRY ANALYSIS

To describe the complex character of changing the vortex core structure let us use symmetry arguments in line with the phase-transition theory of Landau. For both observed critical values of anisotropy, when the symmetry of state changes significantly. At $\beta \geq \beta_1$, when the out-of-plane core emerges for the first time, the sign of M_z can be arbitrary; i.e., there is a spontaneous breaking of Z_2 symmetry with respect to M_z at $\beta = \beta_1$. In contrast to that, the symmetry of the planar distribution of magnetic moments does not change at this transition point: within the range $\beta_1 < \beta < \beta_2$ it remains the same as for $\beta < \beta_1$. At the other transition point $\beta = \beta_2$ the situation is different: the dependence of the out-of-plane component $M_z(\beta)$ does not have any visible peculiarities, while the planar component M_{pl} vanishes at $\beta = \beta_2$ and remains zero for $\beta_2 \leq \beta \leq \beta_t$, i.e., up to the point of destruction of the vortex state at $\beta = \beta_t$; see the detailed graph in Fig. 5.

For the ground state in the interval $\beta_2 \leq \beta \leq \beta_t$, we observe a higher symmetry of the moment distribution than the vortex states with $M_{pl} \neq 0$ at $\beta < \beta_2$ (specifically, within

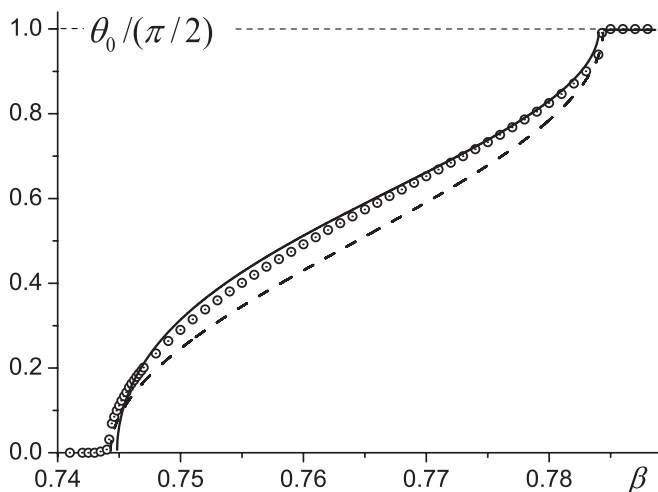


FIG. 6. The value of the angle θ_0 (normalized by $\pi/2$) vs the anisotropy constant β for a cluster with 61 particles in the region of the vortex core reconstruction. Symbols present the results of numerical calculations, while the dashed and solid lines show analytical results from the phenomenological theory. The dashed line corresponds to Eq. (3), and the solid line shows the result that follows from including corrections due to the sixth-order term with $\bar{\beta}$; see the text.

the numerical accuracy of our simulations, we observe the C_6 symmetry; it would be worth finding out whether this symmetry is exact). Rather low symmetry of the vortex ground state at $\beta < \beta_2$ is caused by the presence of nonzero M_{pl} , which can be traced to the presence of a nonzero planar component of the central magnetic moment $\vec{\mu}_0$. Obviously, the emergence of nonzero M_z at $\beta > \beta_1$ is caused by $\vec{\mu}_0$ coming out of the plane. Writing down $\vec{\mu}_0$ as $\vec{\mu}_0 = \mu_0(\sin \theta_0 \vec{e}_z + \cos \theta_0 \vec{e}_{pl})$, where \vec{e}_{pl} lies in the plane of the system, we find that the transition at β_1 is connected to the appearance of nonzero θ_0 , with $\theta_0 = 0$ at $\beta \leq \beta_1$ and $\theta_0 \neq 0$ at $\beta > \beta_1$. As we pointed out, the symmetry of the state with $M_z \neq 0$ is lower than for a planar vortex; therefore the value of θ_0 serves as the order parameter for the transition at $\beta = \beta_1$. In this case, one can expect that at $\beta \geq \beta_1$ the behavior of the “order parameter” close to the transition is given by $\theta_0 \propto \sqrt{\beta - \beta_1}$ and is characterized by singular behavior, $d\theta_0/d\beta \rightarrow \infty$ at $\beta \rightarrow \beta_1 + 0$. On the other hand, the hexagonal symmetry in the spin distribution may appear only when the central moment is directed strictly perpendicular to the system plane, i.e., at $\theta_0 = \pi/2$. If at $\beta = \beta_2$ the symmetry increases up to the hexagonal one, the quantity $\vartheta_0 = \pi/2 - \theta_0$ should serve as the order parameter for this transition. We arrive at the conclusion that the behavior of the out-of-plane component of the central spin $\vec{\mu}_0$, i.e., the dependence $\theta_0(\beta)$, dictates the change of symmetry of the vortex state. Information about the full $\theta_0(\beta)$ dependence can be obtained only numerically, but the presence of square-root singularities at $\beta \rightarrow \beta_1 + 0$ and $\beta \rightarrow \beta_2 - 0$ is rather easily verified (see Fig. 6).

The detailed analysis of the $\theta_0(\beta)$ dependence allows one to present a closed phenomenological expression for the “thermodynamic potential” Φ that defines the behavior of $\theta_0(\beta)$ in a wide range of β . Indeed, in line with the Landau theory, this potential can be constructed in the form of the expansion in powers of the order parameters, which are θ_0

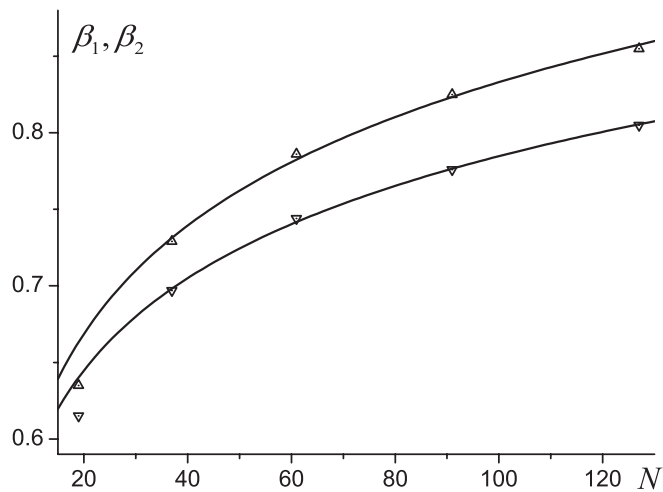


FIG. 7. The dependence of β_2 (up triangles) and β_1 (down triangles) on the number of particles in the cluster, lines present the dependence fitted by the logarithmic function, see the text.

at $\beta \simeq \beta_1$ or $\vartheta_0 = \pi/2 - \theta_0$ at $\beta \simeq \beta_2$. Equivalently, $\sin \theta_0$ and $\cos \theta_0$ can be used instead of angles θ_0 and ϑ_0 . As odd degrees of $\mu_{0z} = \sin \theta_0$ are forbidden by the condition of the time reversal invariance, and the simplest form of this energy is the following: $\Phi = A \sin^2 \theta_0 + B \sin^4 \theta_0$. It is easy to see that, up to an inessential overall factor, the correct behavior is provided by the expression

$$\Phi = \frac{1}{2} (\beta_1 - \beta) \sin^2 \theta_0 + \frac{1}{4} (\beta_2 - \beta_1) \sin^4 \theta_0, \quad (2)$$

which leads to the simple result:

$$\sin \theta_0 = \sqrt{\frac{\beta - \beta_1}{\beta_2 - \beta_1}}, \quad \beta_1 \leq \beta \leq \beta_2, \quad (3)$$

while $\theta_0 = 0$ at $\beta < \beta_1$, and $\theta_0 = \pi/2$ at $\beta > \beta_2$.

Such simple dependence describes the numerical data fairly well, see Fig. 6. Deviation from the simple law given by (3) can be accounted for by adding the term $(\bar{\beta}/6) \sin^6 \theta_0$ to the expansion (2). As seen from Fig. 6, it provides a perfect description of the numerical data at sufficiently small $\bar{\beta}$, typical values are $\bar{\beta} \leq 0.1(\beta_2 - \beta_1)$.

The critical values of the anisotropy constant β_1 and β_2 grow with the increase of the cluster size N , see Fig. 7, though for the studied values of N this dependence is rather slow. The numerical data for $N \geq 37$ can be well fitted by a logarithmic dependence of the form $\beta_{1,2} = A_{1,2} + B_{1,2} \ln N$, where $A_1 = 0.38397$, $B_1 = 0.08703$; $A_2 = 0.36236$, $B_2 = 0.10222$.

The value of θ_0 not only dictates the vortex core symmetry but it also quantitatively defines the important vortex characteristic, the total out-of-plane moment of the particle with the vortex. Singularities in the θ_0 behavior at $\beta = \beta_1$ are reflected in the $M_z(\beta)$ dependence, $M_z \propto \sin \theta_0$ near this point. It is worth noting that M_z plays a special role in the dynamic properties, namely, M_z serves as a proper collective variable describing the radial mode (with the azimuthal number $m = 0$) of the magnetization oscillations in the particle with a vortex;⁵⁷ the theory is in agreement with recent experiment.⁵⁸ Therefore, the presence of singularities in $M_z(\beta)$ should manifest itself in the behavior of an equivalent of this mode for the considered system.

In addition, the presence or absence of the vortex core is also important for the properties of azimuthal modes with $m = \pm 1$.^{4,11–13,59,60} For a purely planar vortex, the modes with $m = \pm 1$ form degenerate doublets, while the emergence of the core leads to splitting of these doublets. Thus, one can expect a crucial impact of the vortex structure modification on the properties of eigenmodes of the vortex-state particle, although a detailed discussion of the dynamical properties of the particle with the vortex is beyond the scope of this work.

IV. SUMMARY AND DISCUSSION

To conclude, we have shown that high-symmetry hexagonal fragments of a 2D closely-packed triangular lattice of magnetic particles contain a vortex in the ground state, even for a small fragment size. The vortex structure is very sensitive to the intrinsic anisotropy β of the particle. At small anisotropy, there is a purely planar vortex. With the increase of β , the symmetry of the vortex ground state lowers initially at some critical value $\beta = \beta_1$, and then increases to a high sixfold axial symmetry above another critical value $\beta = \beta_2 > \beta_1$. It is worth to note that those two transformations bear a similarity to second-order phase transitions. Both transitions take place at sufficiently weak anisotropy, the dimensionless parameters $\beta_{1,2}$ do not exceed one. This value is essentially smaller than the easy-plane anisotropy of a planar array induced by the demagnetization field with the characteristic value $\beta_{\text{array}} \sim 10$, see Ref. 48. Actually, this anisotropy is smaller than it is necessary to create the perpendicular magnetization of a cylindrical magnetic dot.

An important challenge in the physics of magnetic vortices is to find ultra-small (smaller than 100 nm) systems with vortices in the ground state, this problem is of great interest for both fundamental physics and applications. In addition to lithographic magnetic materials, where the particle size is of the order of tens of nanometers,^{53–55} the proposed theory is applicable to other 2D systems with anisotropic particles having magnetic or electrical dipole moment.⁴⁰ One could expect that if an array can be composed from small enough particles, having finite magnetic or electric dipole moment, the vortex state will be present for arrays 10–20 times larger than the particle size. Such systems can be realized for composite magnetic materials, for example, for granular magnets with the content of the magnetic component less than the percolation

threshold, where the exchange interaction between nanometer-sized grains is anomalously small. Another example is the inhomogeneous state arising in the vicinity of the metal–insulator transition in doped manganites, which involves small particles of the ferromagnetic (metallic) phase distributed over a nonmagnetic host; their physical properties are determined to a large extent by the dipolar interactions between these particles.⁶¹ The experimental implementation of the artificial crystals, in which particles with magnetic moments of the order of 10^3 Bohr magnetons form an ordered lattices, has been reported recently.⁶² As one more example, it is instructive to mention a new class of materials, namely, molecular crystals formed by high-spin molecules. The total magnetic moment of such a molecule can be as high as dozens of Bohr magnetons, but the exchange interaction between magnetic moments of different molecules is almost negligible.⁶³ Note also so-called dense phases formed by nanometer-sized magnetic particles moving freely in a liquid (that is the standard situation for a ferrofluids).⁶⁴ For all these systems with a particle size of the order of nanometers the vortices described here can be present for objects as small as dozen of nanometers; those are, to the best of our knowledge, the smallest vortex-bearing systems discussed in the literature.

It is worth noting that the presence of a vortex ground state for such small systems and the transitions with the vortex core reconstruction is a consequence of the high (hexagonal) symmetry of the array. For square or rectangular arrays the vortex state appears for large enough arrays only.⁵¹ As we found, for an array shaped as a regular triangle, the vortex state could be present for small arrays, but with the increase of the anisotropy the vortex remain coreless all the way till the transition to antiferromagnetic state. The two-dimensional nature of an array is also quite important. Thus, two-dimensional closely-packed arrays of magnetic particles represent vortex-bearing systems with potentially small sizes and offer a unique possibility for manipulating the symmetry and structure of the vortex core.

ACKNOWLEDGMENTS

We thank V. G. Baryakhtar, A. K. Kolezhuk, and V. F. Kovalenko for useful discussions. This work was partly supported by the government of Ukraine, state program “Nanotechnologies and Nanomaterials,” Project No. 1.1.3.27.

*bivanov@i.com.ua

¹R. Skomski, *J. Phys. Condens. Matter* **15**, R841 (2003); *Advanced Magnetic Nanostructures*, edited by D. J. Sellmyer and R. Skomski, (Springer, New York, 2006).

²R. Antos, Y. Otani, and J. Shibata, *J. Phys. Soc. Jpn.* **77**, 031004 (2008).

³K. Yu. Guslienko, *J. Nanosci. Nanotechnol.* **8**, 2745 (2008).

⁴B. A. Ivanov, H. J. Schnitzer, F. G. Mertens, and G. M. Wysin, *Phys. Rev. B* **58**, 8464 (1998).

⁵F. G. Mertens and A. R. Bishop, in *Nonlinear Science at the Dawn of the 21st Century*, edited by P. L. Christiansen and M. P. Soerensen (Springer, Berlin, 1999), pp. 137–170.

⁶G. E. Volovik and V. P. Mineev, *Zh. Eksp. Teor. Fiz.* **72**, 2256 (1977) [*Sov. Phys. JETP* **45**, 1186 (1977)].

⁷N. D. Mermin, *Rev. Mod. Phys.* **51**, 591 (1979).

⁸A. M. Kosevich, B. A. Ivanov, and A. S. Kovalev, *Phys. Rep.* **194**, 117 (1990); *Phys. D* **3**, 363 (1981).

⁹S. Gliga, M. Yan, R. Hertel, and C. M. Schneider, *Phys. Rev. B* **77**, 060404 (2008).

¹⁰G. M. Wysin, *Phys. Lett. A* **240**, 95 (1998); *Phys. Rev. B* **49**, 8780 (1994).

¹¹B. A. Ivanov and G. M. Wysin, *Phys. Rev. B* **65**, 134434 (2002).

¹²B. A. Ivanov and C. E. Zaspel, *Appl. Phys. Lett.* **81**, 1261 (2002); *J. Appl. Phys.* **95**, 7444 (2004); *Phys. Rev. Lett.* **94**, 027205 (2005).

- ¹³F. Boust and N. Vukadinovic, *Phys. Rev. B* **70**, 172408 (2004).
- ¹⁴C. E. Zaspel, B. A. Ivanov, J. P. Park, and P. A. Crowell, *Phys. Rev. B* **72**, 024427 (2005).
- ¹⁵R. Zivieri and F. Nizzoli, *Phys. Rev. B* **71**, 014411 (2005); **74**, 219901(E) (2006).
- ¹⁶R. Zivieri and F. Nizzoli, *Phys. Rev. B* **78**, 064418 (2008).
- ¹⁷X. Zhu, Z. Liu, V. Metlushko, P. Grutter, and M. R. Freeman, *Phys. Rev. B* **71**, 180408 (2005).
- ¹⁸S.-B. Choe, Y. Acremann, A. Scholl, A. Bauer, A. Doran, J. Stöhr, and H. A. Padmore, *Science* **304**, 420 (2004).
- ¹⁹M. Buess, T. P. J. Knowles, R. Höllinger, T. Haug, U. Krey, D. Weiss, D. Pescia, M. R. Scheinfein, and C. H. Back, *Phys. Rev. B* **71**, 104415 (2005).
- ²⁰M. Buess, R. Hoellinger, T. Haug, K. Perzlmaier, U. Krey, D. Pscia, M. R. Scheinfein, D. Weiss, and C. H. Back, *Phys. Rev. Lett.* **93**, 077207 (2004).
- ²¹M. Buess, T. Haug, M. R. Scheinfein, and C. H. Back, *Phys. Rev. Lett.* **94**, 127205 (2005).
- ²²F. Hoffmann, G. Woltersdorf, K. Perzlmaier, A. N. Slavin, V. S. Tiberkevich, A. Bischof, D. Weiss, and C. H. Back, *Phys. Rev. B* **76**, 014416 (2007).
- ²³B. A. Ivanov and C. E. Zaspel, *Phys. Rev. Lett.* **99**, 247208 (2007).
- ²⁴V. S. Pribiag, I. N. Krivorotov, G. D. Fuchs, P. M. Braganca, O. Ozatay, J. C. Sankey, D. C. Ralph, and R. A. Buhrman, *Nat. Phys.* **3**, 498 (2007).
- ²⁵A. V. Khvalkovskiy, J. Grollier, A. Dussaux, K. A. Zvezdin, and V. Cros, *Phys. Rev. B* **80**, 140401(R) (2009).
- ²⁶Y. S. Choi, K. S. Lee, and S. K. Kim, *Phys. Rev. B* **79**, 184424 (2009).
- ²⁷Q. Mistral, M. van Kampen, G. Hrkac, J.-V. Kim, T. Devolder, P. Crozat, C. Chappert, L. Lagae, and T. Schrefl, *Phys. Rev. Lett.* **100**, 257201 (2008); A. Dussaux, B. Georges, J. Grollier, V. Cros, A. V. Khvalkovskiy, A. Fukushima, M. Konoto, H. Kubota, K. Yakushiji, S. Yuasa, K. A. Zvezdin, K. Ando, and A. Fert, *Nat. Commun.* **1**, 8 (2010).
- ²⁸B. A. Ivanov, G. G. Avanesyan, A. V. Khvalkovskiy, N. E. Kulagin, C. E. Zaspel, and K. A. Zvezdin, *JETP Lett.* **91**, 178 (2010).
- ²⁹S. S. Cherepov, B. C. Koop, A. Yu. Galkin, R. S. Khymyn, B. A. Ivanov, D. C. Worledge, and V. Korenivski, *Phys. Rev. Lett.* **109**, 097204 (2012).
- ³⁰S. M. Mohseni, S. R. Sani, J. Persson, T. N. Anh Nguyen, S. Chung, Ye. Pogoryelov, P. K. Muduli, E. Iacocca, A. Eklund, R. K. Dumas, S. Bonetti, A. Deac, M. A. Hofer, and J. Akerman, *Science* **339**, 1295 (2013).
- ³¹V. V. Kruglyak, S. O. Demokritov, and D. Grundler, *J. Phys. D* **43**, 264001 (2010).
- ³²R. Hertel, W. Wulfhekel, and J. Kirschner, *Phys. Rev. Lett.* **93**, 257202 (2004); S. Choi, K.-S. Lee, K. Y. Guslienko, and S.-K. Kim, *ibid.* **98**, 087205 (2007); S. Neusser and D. Grundler, *Adv. Mater.* **21**, 2927 (2009).
- ³³V. E. Kireev and B. A. Ivanov, *JETP Lett.* **94**, 306 (2011).
- ³⁴D. A. Dimitrov and G. M. Wysin, *Phys. Rev. B* **50**, 3077 (1994); **51**, 11947 (1995).
- ³⁵V. E. Kireev and B. A. Ivanov, *Phys. Rev. B* **68**, 104428 (2003).
- ³⁶J. M. Luttinger and L. Tisza, *Phys. Rev.* **70**, 954, (1946).
- ³⁷P. I. Belobrov, R. S. Gekht, and V. A. Ignatchenko, *Zh. Eksp. Teor. Fiz.* **84**, 1097 (1983) [*Sov. Phys. JETP* **57**, 636 (1983)].
- ³⁸J. G. Brankov and D. M. Danchev, *Phys. A* **144**, 128 (1987); S. Prakash and C. L. Henley, *Phys. Rev. B* **42**, 6574 (1990).
- ³⁹K. Yu. Guslienko, *Appl. Phys. Lett.* **75**, 394 (1999).
- ⁴⁰V. M. Rozenbaum, V. M. Ogenko, and A. A. Chuiko, *Sov. Phys. Usp.* **34**, 883 (1991).
- ⁴¹J. E. L. Bishop, A. Yu. Galkin, and B. A. Ivanov, *Phys. Rev. B* **65**, 174403 (2002).
- ⁴²A. Yu. Galkin and B. A. Ivanov, *JETP Lett.* **83**, 383 (2006).
- ⁴³I. R. Karetnikova, I. M. Nefedov, M. V. Sapozhnikov, A. A. Fraerman, and I. A. Shereshevskii, *Phys. Solid State* **43**, 2115 (2001).
- ⁴⁴P. Politi and M. G. Pini, *Phys. Rev. B* **66**, 214414 (2002).
- ⁴⁵A. Yu. Galkin, B. A. Ivanov, and C. E. Zaspel, *Phys. Rev. B* **74**, 144419 (2006).
- ⁴⁶L. Giovannini, F. Montoncello, and F. Nizzoli, *Phys. Rev. B* **75**, 024416 (2007).
- ⁴⁷E. Tartakovskaya, W. Kreuzpaintner, and A. Schreyer, *J. Appl. Phys.* **103**, 023913 (2008).
- ⁴⁸P. V. Bondarenko, A. Yu. Galkin, B. A. Ivanov, and C. E. Zaspel, *Phys. Rev. B* **81**, 224415 (2010).
- ⁴⁹B. A. Ivanov and V. E. Kireev, *JETP Lett.* **90**, 750 (2009).
- ⁵⁰B. A. Ivanov, *Low Temp. Phys.* **31**, 635 (2005) [*Fiz. Nizk. Temp.* **31**, 841 (2005)].
- ⁵¹P. Politi, M. G. Pini, and R. L. Stamps, *Phys. Rev. B* **73**, 020405(R) (2006).
- ⁵²N. A. Usov and S. E. Peschany, *J. Magn. Magn. Mater.* **135**, 111 (1994).
- ⁵³S. Y. Chou, M. S. Wei, P. R. Krauss, and P. B. Fischer, *J. Appl. Phys.* **76**, 6673 (1994).
- ⁵⁴G. Meier, M. Kleiber, D. Grundler, D. Heitmann, and R. Wiesendanger, *Appl. Phys. Lett.* **72**, 2168 (1998).
- ⁵⁵C. A. Ross, M. Hwang, M. Shima, J. Y. Cheng, M. Farhoud, T. A. Savas, H. I. Smith, W. Schwarzacher, F. M. Ross, M. Redjfal, and F. B. Humphrey, *Phys. Rev. B* **65**, 144417 (2002).
- ⁵⁶M. E. J. Newman and G. T. Barkema, *Monte Carlo Methods in Statistical Physics* (Oxford University Press, New York, 1999).
- ⁵⁷C. E. Zaspel, E. S. Wright, A. Yu. Galkin, and B. A. Ivanov, *Phys. Rev. B* **80**, 094415 (2009); A. Yu. Galkin and B. A. Ivanov, *J. Exp. Theor. Phys.* **109**, 74 (2009) [*Zh. Eksp. Teor. Fiz.* **136**, 87 (2009)].
- ⁵⁸V. Castel, J. Ben Youssef, F. Boust, R. Weil, B. Pigeau, G. de Loubens, V. V. Naletov, O. Klein, and N. Vukadinovic, *Phys. Rev. B* **85**, 184419 (2012).
- ⁵⁹G. M. Wysin, *Phys. Rev. B* **54**, 15156 (1996).
- ⁶⁰G. M. Wysin and W. Figueiredo, *Phys. Rev. B* **86**, 104421 (2012).
- ⁶¹V. N. Krivoruchko, M. A. Marchenko, and Y. Melikhov, *Phys. Rev. B* **82**, 064419 (2010).
- ⁶²O. Kasyutich, R. D. Desautels, B. W. Southern, and J. van Lierop, *Phys. Rev. Lett.* **104**, 127205 (2010).
- ⁶³W. Wernsdorfer, *Adv. Chem. Phys.* **118**, 99 (2001).
- ⁶⁴R. E. Rosensweig, *Ferrohydrodynamics* (Cambridge University Press, Cambridge, 1985; Russian translation by Mir, Moscow, 1989).